International Journal of Heat and Mass Transfer 52 (2009) 1552–1560

Contents lists available at ScienceDirect

International Journal of Heat and Mass Transfer

journal homepage: www.elsevier.com/locate/ijhmt

An experimental investigation of the effect of longitudinal fin orientation on heat transfer in membrane water wall tubes in a circulating fluidized bed

Anusorn Chinsuwan [a,1], Animesh Dutta [b,*]

[a] Energy Field of Study, School of Environment, Resources and Development, Asian Institute of Technology, Klong Luang, Pathumthani 12120, Thailand
[b] Engineering Department, Nova Scotia Agricultural College, P.O. Box 550, Truro, NS, Canada B2N 5E3

ARTICLE INFO

Article history:
Received 19 December 2007
Received in revised form 7 August 2008
Available online 26 September 2008

Keywords:
Circulating fluidized bed
Membrane water wall tube
Finned tube
Heat transfer coefficient

ABSTRACT

Experiments were conducted in a cold model circulating fluidized bed having riser cross-sectional area of 100 mm × 100 mm, height of 4.8 m, bed temperature of 75 °C and superficial velocity of 8 m s^{-1}. Local sand having average diameter of 231 μm was used as bed material. The experiments were conducted for three tube configurations: membrane tube, membrane tube with a longitudinal fin at the tube crest and membrane tube with two longitudinal fins at 45° on both sides of the tube crest. The results show that membrane tubes with one and two longitudinal fins have higher heat transfer than membrane tubes and the heat is mainly transferred in the combination portion of tube and membrane fins. In addition, the membrane tube has the highest heat transfer coefficient.

1. Introduction

Circulating fluidized bed (CFB) boilers are widely used for power generation due to their low pollution, fuel flexibility and high combustion efficiency. However, the design methodology is not as well established as that of pulverized coal fired boilers [1].

CFB boilers operate in the fast fluidized bed regime where the majority of particles at the bulk bed temperature move upwards through the core of the furnace and flow downwards along the membrane water wall tubes of the CFB boiler in the form of cluster of particles or strands. The heated particles slide along the surface of the wall for a certain distance after that they separate from the wall and mix with the bulk of the bed. As they slide along the wall, they transfer their heat to the wall. This causes their temperatures and the heat transfer rate to decrease as the traveling distance of the particles increases. This mode of heat transfer plays the most important role in heat transfer from the bed to water wall tubes and is called particle convection [2,3]. According to the heat transfer mechanism, the heat transfer can be increased if there are more renewal particles which come in contact with the wall. At elevated temperature, radiation contributes to the heat transfer both to the covered and uncovered surfaces by the particles. By visual observations on the wall of a 12 MW_{th} CFB boiler, Golriz [4] reported that there was higher particle concentration over the fins than the tube crests. In addition, they traveled on the fins longer than those traveling on the tube crests. A combination of longer residence time of particles on and the lower view factor of the fin leads to lower heat transfer coefficients on the fin.

To maintain the combustion temperature at an optimum level in a CFB boiler, it is required for the water tube walls of a CFB furnace to absorb a certain fraction of the heat input to the furnace. In addition, high capacity CFB boilers having high heat inputs are required to have additional heating surfaces either across the furnace or external heat exchangers. However, the both options are not only costly but also risk to erosion.

To fill this gap in research knowledge related to heat transfer in the CFB loop, a series of research on heat transfer to the wing walls [5,6], to the standpipes [7], to the cavity type inertial separators [8] and to the ceiling of the riser of a CFB boiler [9] was conducted. In this present work, a study of enhancement of heat absorption by the membrane water wall is conducted.

Longitudinal fins welded on membrane water wall tubes may provide additional heat absorption in CFB furnace. In addition, this concept has the following advantages: it may help reduce erosion of the water wall because the fins may reduce particle momentum; it increases the area moment of inertia of the tube; it is simple to manufacture and less costly; and it may be added to the water wall of an existing boiler [10].

As reviewed by Basu and Nag [2], a number of investigators have investigated heat transfer in CFB risers. Some of these are presented in Table 1. Reddy and Nag [12] reported that the addition of a longitudinal fin to membrane tube at the tube crest leads to an increase in the heat absorption from bed to wall but results in a drop in the heat transfer coefficient. An increase in heat absorption up to 45% is found in the work of Basu and Cheng [10]. Since the fact that fin efficiency increases with a decrease in fin height, for the same surface area, heat transfer might be improved by adding

* Corresponding author. Tel.: +1 902 8936711; fax: +1 902 8931859.
E-mail addresses: anuchi@kku.ac.th (A. Chinsuwan), adutta@nsac.ca (A. Dutta).
[1] Present address: Mechanical Engineering Department, Faculty of Engineering, Khon Kaen University, Thailand.

0017-9310/$ - see front matter © 2008 Elsevier Ltd. All rights reserved.
doi:10.1016/j.ijheatmasstransfer.2008.08.005

Nomenclature

A	area (m^2)
CFB	circulating fluidized bed
c	specific heat capacity ($J\,kg^{-1}\,°C^{-1}$)
d	test tube diameter, diameter (m and μm for particle size)
EL	elevation
G	circulating rate ($kg\,m^{-2}\,s^{-1}$)
g	gravity acceleration ($m\,s^{-2}$)
H	test tube length, height (m)
h	heat transfer coefficient ($W\,m^{-2}\,°C^{-1}$)
hA	heat transfer capacity ($W\,°C^{-1}$)
I	bed inventory (kg)
ID	inside diameter (m)
k	thermal conductivity ($W\,m^{-1}\,°C^{-1}$)
L	longitudinal fin height (m)
$\dot{m}$	mass flow rate ($kg\,s^{-1}$)
m	fin constant (m^{-1})
p	pressure (Pa)
P	convection perimeter (m)
Q	heat transfer rate (W)
r	tube radius (m)
T	temperature, temperature distribution along fin height (°C)
U	superficial velocity ($m\,s^{-1}$)
x	distance from fin base (m)

Subscripts

2lf	longitudinal fin at 45° of tube crest
amb	ambient
avg	based on average
b	bed
c	based on cross-section
i	inner tube
in	inlet
lf	a longitudinal fin at tube crest
mf	membrane fin
o	fin base, outer tube
out	outlet
p	particle, based on constant pressure, tube wall
s	solid, based on surface
T	total
t	tube
tip	fin tip
t–mf	tube and membrane fin portions
w	water

Greek symbols

Δ	difference
ε	voidage (–)
ρ	density, suspension density ($kg\,m^{-3}$)
ω	exposed angle (rad)

shorter longitudinal fins. However, these fins have to be attached around the outside tube surface which might restrict the motion of bed particles on the surface. In addition, a change in fin orientation on the tube might have an affect on the motion of the particles on its surface.

As far as authors are concerned, information on the effect of longitudinal fin orientation on the heat transfer behavior in membrane water wall tubes is lacking. Hence, the aims of this work are to investigate the heat transfer and heat transfer coefficient of membrane water wall tubes, the membrane water wall with a longitudinal fin at the tube crest and with two longitudinal fins at 45° on both sides of the tube crest. In addition, the heat transfer and heat transfer coefficient of the longitudinal fin portion and the combination of the tube and membrane fins portion are also investigated.

2. Experimental setup

The cold model circulation fluidized bed equipment used in this work has a riser height of 4.8 m and 100 mm × 100 mm in cross-section as shown in Fig. 1(a). It is fabricated from carbon steel plate having a thickness of 2.3 mm. The fluidization air is supplied by a high pressure blower through the distributor plate located at the bottom of the riser. The distributor plate is made from 6 mm thickness steel plate. It has holes of diameter 3 mm with 10 mm square pitch. This arrangement corresponds to 7.07% opening fraction. Local sand having bulk density of 1515 $kg\,m^{-3}$, particle density (ρ_s) of 2774 $kg\,m^{-3}$ and average diameter (d_p) of 231μ m is used as bed material. The entrained particles leaving the riser are captured in a cyclone located at the top of the return pipe. The upper portion of the return pipe is made of clear plastic having a diameter of 55 mm. At the bottom of this part, there is a butterfly valve used as a particle measuring valve. The solid circulation rate is measured by closing this valve and measuring the volume of solids collected in this pipe portion for a certain time. In order to have enough bed material to feed the riser when this valve is shut off, there is a storage column made of clear plastic pipe having a diameter of 80 mm located under this valve. Under this part, there is a butterfly valve used as a particle control valve. The bed material from the return pipe is fed into the riser via a pipe having a diameter of 55 mm. Compressed air from a compressor is used as aeration air and supplied to the system at below the material control valve. The aeration air pressure is adjusted by using a pressure regulator. Backflow is controlled by adjusting the aeration pressure and the particle control valve.

The air flow rate in the riser is adjusted by using a bypass valve and its velocity is measured by pitot tube. Before the supplied air enters the distributor plate, it is heated by an electric heater having a capacity of 3 kW. Thirteen wall static pressure taps are provided along the height of the riser and they are connected to water manometers.

The test section has a length of 1200 mm and is installed at 1800 mm above the distributor plate. Inside this section there are three types of test tubes. Their arrangement is shown in Fig. 2(a). The tubes are made from carbon steel having outside diameter and thickness of 31.8 mm and 6.5 mm, respectively. The fins have a thickness of 3 mm. In all cases, the test tube has the length of 1000 mm and the height of the membrane fin is 14 mm. T-type thermocouples are spot welded to the temperature measuring points. Details of the test section and details of the test tubes are shown in Fig. 2(b) and Table 2, respectively.

Water at room temperature is pumped from a storage tank and supplied to the test tubes. The water flow rate of each test tube can be adjusted by individual flow control valve and the flow rate can be read from individual water rotameters. At the entrance and exit of the test tubes, thermocouples are installed for measuring the temperature of those points. The water flow diagram is shown in Fig. 1(b).

In order to ensure that the test tubes were under the same hydrodynamic conditions, the test section was arranged in such a way that the tube being tested was on the same side of the riser as shown in Fig. 1.

Table 1
Details of experimental studies on heat transfer in the laboratory CFB units

Authors	Test section			Longitudinal fin			Test conditions					
	d (mm)	H (mm)	L_{mf} (mm)	No. of fin	L_{lf} (mm)	Fin orient.	CFB riser	d_p (μm)	ρ_s (kg m^{-3})	ρ (kg m^{-3})	U (m s^{-1})	G_s (kg m^{-2} s^{-1})
Lockhart et al. [11]	19	914	4.75	na.	na.	na.	152 mm dia. × 9.3 m, cold model	200	2650	25–91	7	33–68
	32	914	8	na.	na.	na.						
Reddy and Nag [12]	34	304	5	na.	na.	na.	102 mm × 102 mm × 5 m, T_b = 380–650 °C	260	2350	<20		
	34	304	5	1	5	tube crest						
Basu and Cheng [10]	50.8	3740	12.7	1	20	tube crest	1600 mm × 680 mm × 9 m, T_b = 722–921 °C		2500	3.42–8.67	4.3–6.5	
Molerus [13]	28	500		na.	na.	na.	190 mm dia × 10 m, T_b = 20–880 °C	194		10–80		
Wu et al. [14]	12.7	1220		na.	na.	na.	152 mm dia. × 9.3 m, T_b = 340–880 °C	188–356	3066	5–70	6.6–9.5	
Furchi et al. [15]	72 mm dia. water jackets			na.	na.	na.	72 mm dia. × 6 m, T_b < 250 °C	269			5.8–12.8	<80
Basu and Ngo [16]	34	304	5	na.	na.	na.	102 mm × 102 mm × 5 m, T_b = 380–650 °C	260	2350	1		
Sekthira et al. [17]	10	800		na.	na.	na.	880 mm dia. × 1.72 m, T_b = 200–350 °C	300, 500	2500	8–160	5–12	
Luan et al. [18]	21.3	1626	6.4	na.	na.	na.	152 mm × 152 mm × 7.3 m, T_b = 800–900 °C	286	2596	10–70	7	
Nag et al. [19]	100 mm dia. × 300 mm with electric heater			4,8	23		100 mm dia. × 5.15 m, cold model, T_b = 66.5–91.59 °C	310	2350	18–76	5.6–11.4	
Present work	31.8	1000	14	See Table 2			100 mm × 100 mm × 4.8 m, cold model, T_b = 39.7–74.9 °C	231	2447	25–75	8	22–110

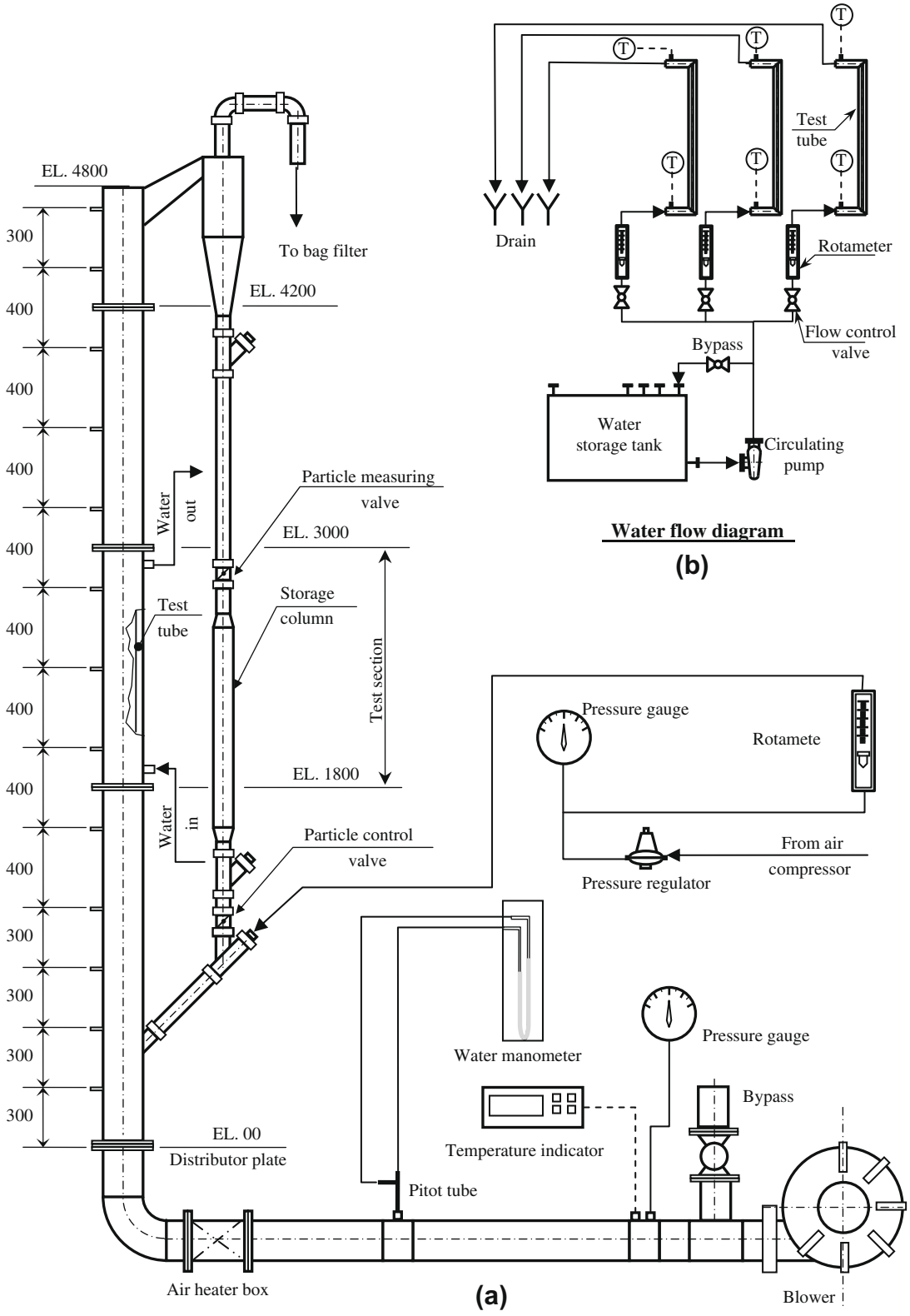

Fig. 1. Schematic diagram of the cold model circulating fluidized bed (all dimensions are in millimeters).

3. Theoretical analysis

3.1. Hydrodynamics

The cross-sectional average voidage (ε) in a riser is determined by following equation:

$$\varepsilon = 1 - \frac{\Delta p}{\rho_s g \Delta H} \tag{1}$$

where Δp is the pressure difference across the two taps, ΔH is the distance between the two wall pressure taps, ρ_s is solid particle density and g is gravity acceleration.

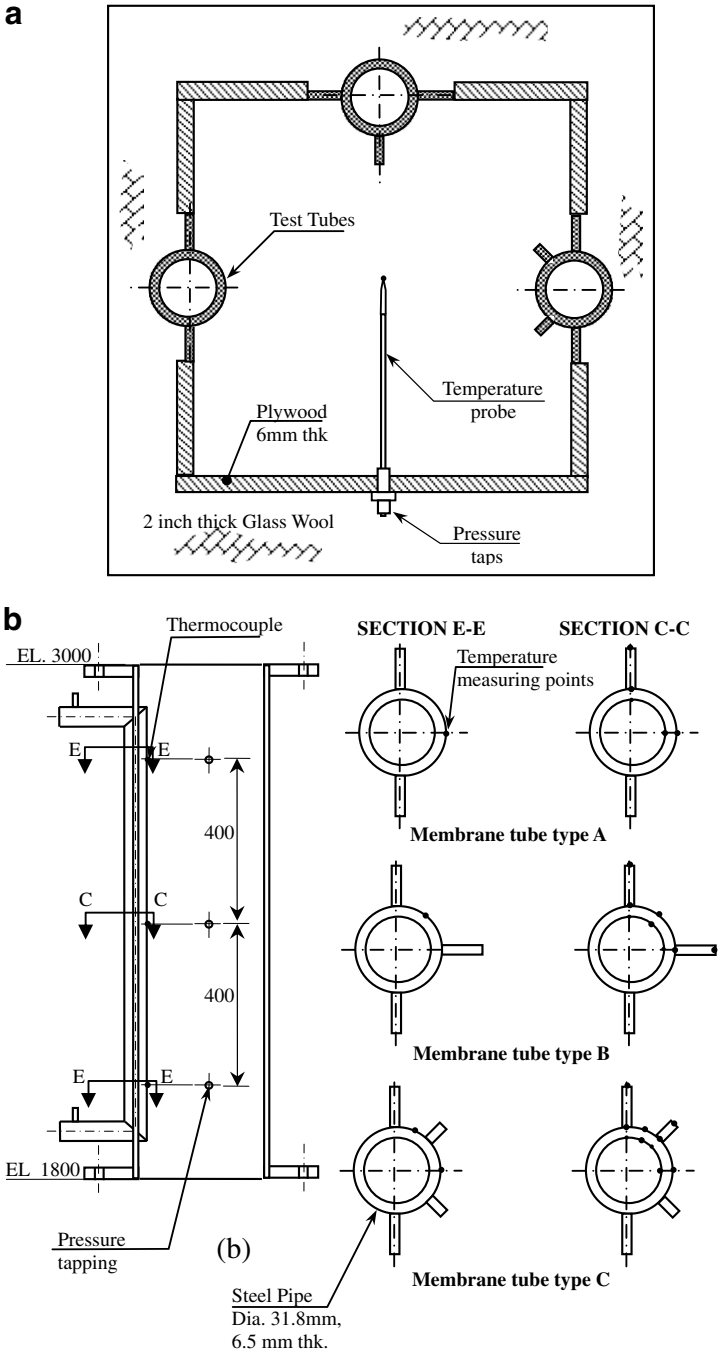

Fig. 2. Arrangement of the test tubes in the test section and details of the test tubes.

The cross-sectional average suspension density (ρ) can be determined as follows:

$$\rho = (1-\varepsilon)\rho_s \tag{2}$$

3.2. Heat transfer

Total heat transfer rate through the test tubes (Q_T) can be calculated from the increase in water energy as

$$Q_T = \dot{m}_w c_p (T_{w,out} - T_{w,in}) \tag{3}$$

where $\dot{m}_w$, c_p, $T_{w,out}$ and $T_{w,in}$ are water mass flow rate, specific heat capacity of water, outlet and inlet water temperatures, respectively.

Alternatively, the total heat transfer can be calculated from the summation of the heat conduction in membrane fins (Q_{mf}), heat conduction across the tube wall (Q_p) and heat conduction in the longitudinal fin (Q_{lf}) [18].

$$Q_T = Q_{mf} + Q_p + Q_{lf} \tag{4}$$

Assuming one-dimensional heat conduction and neglecting heat loss at the fin tip, the temperature distribution (T) along the longitudinal fin height is [20]:

Table 2
Details of the test tubes

Type	Description	Longitudinal fin		
		No. of fins	Height (mm)	Orientation from the tube crest (°)
A	Membrane tube			
B	Membrane tube with a longitudinal fin at the tube crest	1	14	0
C	Membrane tube with two longitudinal fins at both sides of the tube crest	2	7	45

$$\frac{T-T_b}{T_{o,lf}-T_b}=\frac{\cosh m_{lf}(L_{lf}-x)}{\cosh m_{lf}L_{lf}} \tag{5}$$

where, T_b and $T_{o,lf}$ are bed and fin base temperatures, respectively, x is the distance from fin base, L_{lf} is the longitudinal fin height and m_{lf} is the fin constant which is defined as

$$m_{lf}^2=\frac{h_{lf}P}{A_c k} \tag{6}$$

where, h_{lf}, A_c and k are average heat transfer coefficients of the longitudinal fin, cross-sectional area and thermal conductivity of the fin. P is the convection perimeter.

Heat transfer rate in the longitudinal fin (Q_{lf}) can be determined as following:

$$Q_{lf}=(T_b-T_{o,lf})A_c k m_{lf}\tanh(m_{lf}L_{lf}) \tag{7}$$

The nomenclature of a membrane tube with a longitudinal fin is shown in Fig. 3. By knowing the fin base temperature ($T_{o,lf}$) and the temperature at the fin tip ($T_{tip,lf}$), the longitudinal fin constant can be determined according to Eq. (5) as follows:

$$m_{lf}=\frac{1}{L_{lf}}\cosh^{-1}\left[\frac{T_{o,lf}-T_b}{T_{tip,lf}-T_b}\right] \tag{8}$$

For a portion of tube having exposed angle of ω, inside radius of r_i, outside radius of r_o and length of H, heat transfer through the tube thickness can be determined as follows:

$$Q_p=\omega H k\frac{T_{p,o}-T_{p,i}}{\ln(r_o/r_i)} \tag{9}$$

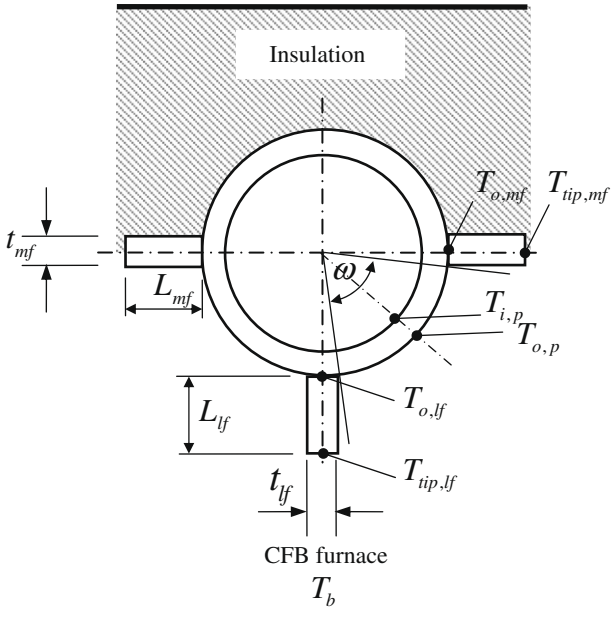

Fig. 3. Nomenclature of a membrane water wall tube with longitudinal fin.

The average heat transfer coefficient of bed to water wall (h_{avg}) is determined as

$$h_{avg}=\frac{Q_T}{A_s(T_b-T_s)} \tag{10}$$

where A_s is the total surface area which is the summation of the area of membrane fin ($A_{s,mf}$), tube ($A_{s,t}$) and longitudinal fin portion ($A_{s,lf}$).

$$A_s=A_{s,mf}+A_{s,t}+A_{s,lf} \tag{11}$$

T_s is the weighted-average exposed surface temperature of the tube and fins which can be estimated as [18]

$$T_s=\frac{A_{s,mf}(T_{o,mf}+T_{tip,mf})/2+A_{s,t}T_{o,p}+A_{s,lf}(T_{o,lf}+T_{tip,lf})/2}{A_{s,mf}+A_{s,t}+A_{s,lf}} \tag{12}$$

For the heat transfer coefficient of the combination of tube and membrane fins portion (h_{t-mf})

$$h_{t\text{-}mf}=\frac{Q_T-Q_{lf}}{A_s(T_b-T_s)} \tag{13}$$

where Q_{lf} is the heat transfer from the longitudinal fin portion which can be determined by using Eq. (7). In this case

$$A_s=A_{s,mf}+A_{s,t} \tag{14}$$

and

$$T_s=\frac{A_{s,mf}(T_{o,mf}+T_{tip,mf})/2+A_{s,t}T_{o,p}}{A_{s,mf}+A_{s,t}} \tag{15}$$

The average heat transfer coefficient of the longitudinal fin (h_{lf}) can be determined from Eqs. (6) and (8) as

$$h_{lf}=\left[\frac{1}{L_{lf}}\cosh^{-1}\left(\frac{T_{o,lf}-T_b}{T_{tip,lf}-T_b}\right)\right]^2\frac{A_c k}{P} \tag{16}$$

4. Experimental uncertainty

A digital data logger was used as a temperature indicator. The thermocouples and logger were calibrated using an oil bath and a standard thermometer. The logger and the thermocouples together have an accuracy of ±0.1 °C. Rotameters having an accuracy of 1% were used to measure the water mass flow rate through the test tubes.

The root of the sum of the square (RSS) [21] was used to estimate the experimental uncertainty. Based on Eqs. (3), (10) and (16), the uncertainties in measured heat transfer rate, average heat transfer coefficient and heat transfer coefficient of the longitudinal fin were 5%, 12% and 8%, respectively.

An additional test was performed to estimate heat loss through the test section. The test was performed by supplying only air at 75 °C with velocity of 8 m s^{-1} through the riser. The heat loss was estimated by balancing the decrease in energy of air across the test section and total heat gained by water in the test tubes. The heat loss was found to be 3%.

5. Results and discussion

Experiments on the three test tubes were conducted under the same hydrodynamic conditions. The experimental conditions are shown in Table 3.

Based on the increase in water energy as in Eq. (3), the obtained average heat transfer coefficient (h_{avg}) of the three test tubes as a function of cross-sectional average suspension density (ρ) are shown in Figs. 4–6. Particle convection is the dominating mode of heat transfer between the fluidized bed and the tube walls. In all cases, it is found that the heat transfer coefficients increase as

Table 3
Experimental conditions

Mean particle size, d_p	231 μm
Particle density, ρ_s	2774 kg m^{-3}
Particle bulk density	1515 kg m^{-3}
Superficial velocity, U	8 m s^{-1}
Suspension density, ρ	25–75 kg m^{-3}
Bed inventory, I	15 kg
Solid circulation rate, G_s	22–110 kg m^{-2} s^{-1}
Bed temperature, T_b	70–75 °C

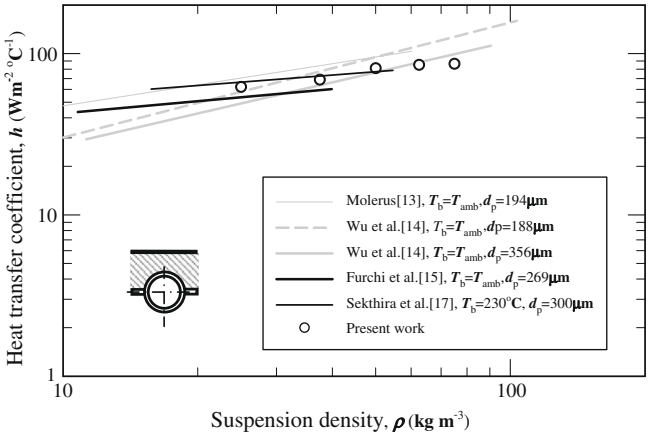

Fig. 4. Heat transfer coefficient of membrane tube (test tube type A).

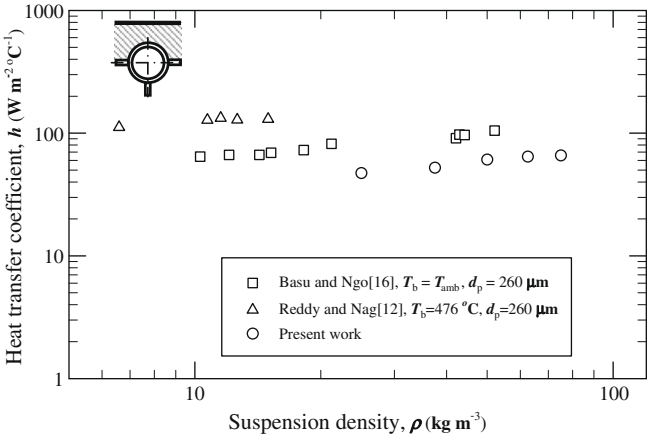

Fig. 5. Heat transfer coefficient of membrane tube with a longitudinal fin at the tube crest (test tube type B).

the suspension density increases. This is because there are more particles coming into contact with the tube wall when the suspension density increases.

The heat transfer coefficients of the tube types A and B are shown in Figs. 4 and 5, respectively. It is seen that their trends are the same as those which others have published in the literature. The difference in heat transfer coefficient is due to the difference in bed temperature and tube length.

The comparison of heat transfer coefficient of the three types of test tube is shown in Fig. 6. It is found that test tube type A has the highest heat transfer coefficient. The tube type C tends to have higher average heat transfer coefficient than the tube type B.

The proposed heat transfer coefficients agree with those which are calculated by using the total heat transfer according to Eq. (4). The comparison is shown in Fig. 7.

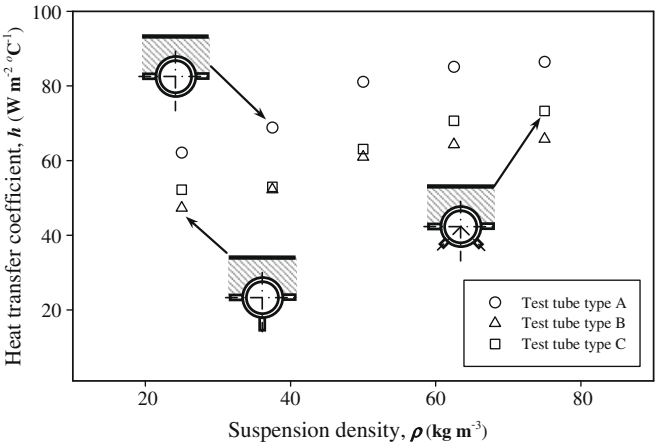

Fig. 6. Comparison of heat transfer coefficient among the type A, B and type C test tubes.

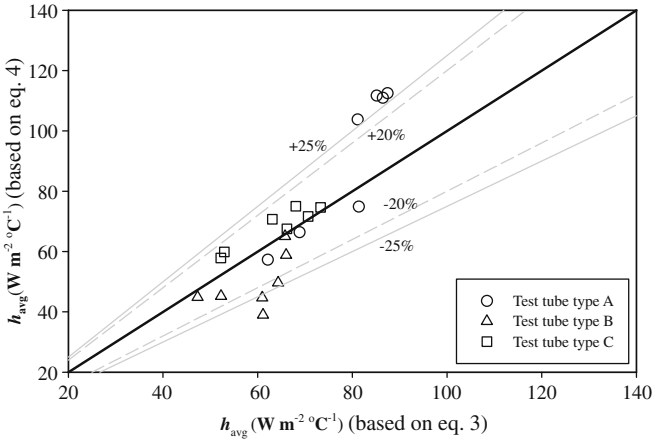

Fig. 7. Comparison of heat transfer coefficients based on an increase in water energy with those based on heat gain by conduction.

With an increase in surface area of 33.36% for tube type B and C compared with that of type A, it is found that the heat transfer ratio of the tube type B to tube type A ($Q_{T,lf}/Q_{T,mf}$) and tube type C to tube A ($Q_{T,2lf}/Q_{T,mf}$) are about 1.25 as shown in Fig. 8. However, the ratio of the average heat transfer coefficient of the tube type B to type A

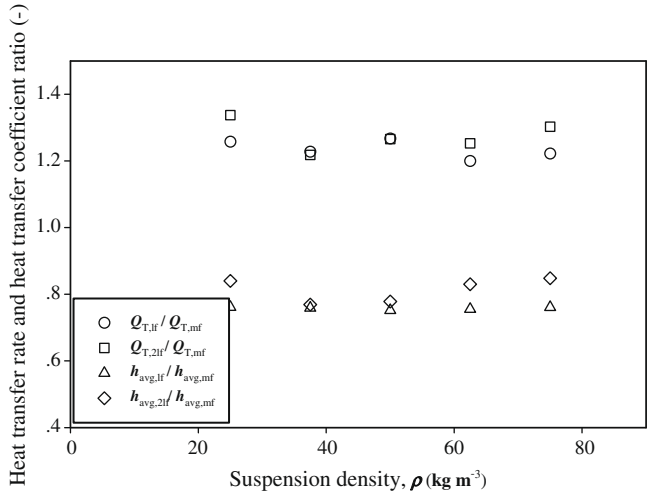

Fig. 8. Comparison of heat transfer and heat transfer coefficient ratio.

($h_{avg,lf}/h_{avg,mf}$) and tube type C to tube A ($h_{avg,2lf}/h_{avg,mf}$) are about 0.75. The trend for an increase in heat transfer rate and a decrease in heat transfer coefficient when adding fins on the heat transfer surface in a circulating fluidized bed was also found in the work of Reddy and Nag [12] and Nag et al. [19]. This is because the longitudinal fins obstruct solid particles which come into contact on the tube's surface which results in decrease in the heat transfer coefficients. The heat transfer rate of the longitudinal finned membrane tubes, tube types B and C, is more than that of the membrane tube because they have more average heat capacity, a product of average heat transfer coefficient and exposed surface area (hA). Membrane fins enhance heat transfer from the bed to fluid inside water wall tubes by collecting heat and transferring it into insulated portions of the tube. This heat transfer rate increases as the tube thickness, fin thickness, fin width and bed side heat transfer coefficient increases [22]. Since there is a decrease in the heat transfer coefficients of the longitudinal finned membrane tubes, the heat transfer from the insulated portion of the tubes is reduced and the increase in heat transfer rate of the tube types B and C is mainly from the exposed portion of the tubes.

As shown in Fig. 9, $Q_{t-mf,lf}/Q_{T,lf}$ and $Q_{t-mf,2lf}/Q_{T,2lf}$ are the ratio of the heat transfer in the combination of tube and membrane fins portion to total heat transfer of the type B and C tubes, respectively. It is found that heat is mainly transferred through the combination of the tube and membrane fins portion. Heat transfer through that portion of the tube for types B and C are 65% and 70%, respectively.

Heat transfer coefficient of the longitudinal fin portion of tubes type B and C (h_{lf} and h_{2lf}), heat transfer coefficient of the combination of tube and membrane fins portion of tubes type B and C ($h_{t-mf,lf}$ and $h_{t-mf,2lf}$) and the average heat transfer coefficient of membrane tube ($h_{avg,mf}$) are shown in Fig. 10. It is found that h_{lf} is higher than h_{2lf}. This indicates that for the tubes having the same configuration as the tubes type B and C, there is more renewal of particles at the tube crest than at 45° from the tube crest. Hence, the heat transfer coefficient of the combination of the tube and membrane fins portion will decrease dramatically if there is any restriction of renewal of particles at the tube crest. Because of this, the heat transfer coefficient of the tube type A ($h_{avg,mf}$) and the tube type B ($h_{t-mf,fl}$) are highest and lowest, respectively. In the case of the tube type C, there is enough space between the two longitudinal fins to ease the particle motion on the tube crest. As a result, $h_{t-mf,2fl}$ is more than $h_{t-mf,fl}$ and it is more sensitive to suspension density than $h_{t-mf,fl}$. When comparing the heat transfer coefficient between the longitudinal fin portion and the combination of tube and membrane fins portion of the same tube type, it is found that

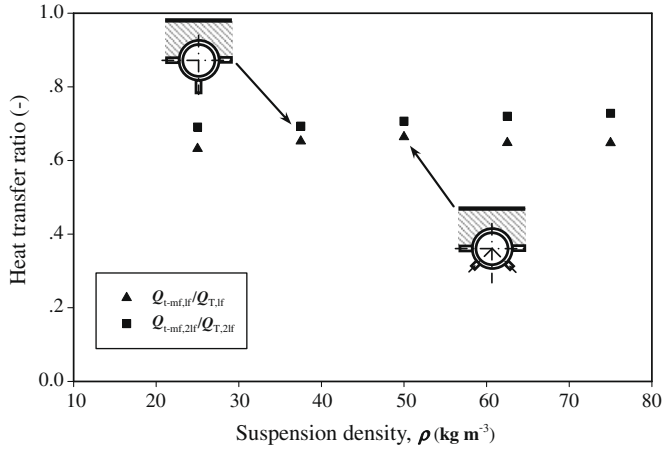

Fig. 9. Heat transfer ratio of the combination of the tube and membrane fins portion to total heat transfer of the type B and C tubes.

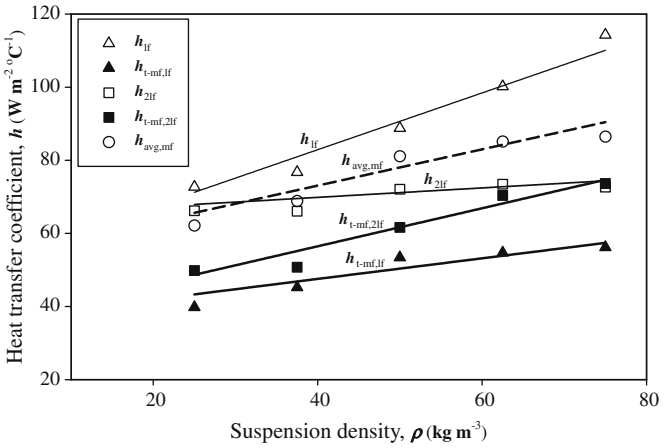

Fig. 10. Comparison of heat transfer coefficient of the fin portion and the combination of the tube and membrane fins portion of the type B and C tubes with the average heat transfer coefficient of the type A tube.

$h_{lf} > h_{t-mf,lf}$ and $h_{2lf} > h_{t-mf,2lf}$. This indicates that there is more renewal of sand particles at the longitudinal fin portion than that at the combination of tube and membrane fins portion.

6. Conclusions

The effect of longitudinal fin orientation on heat transfer in membrane water wall tube was investigated by comparing the heat transfer behavior among the three tube configurations: membrane tube, membrane tube with a longitudinal fin at the tube crest and membrane tube with two longitudinal fins at 45° on both side of the tube crest. In all cases, tube and membrane fins have the same configuration. For the last two, the height of the longitudinal fins of the tube having two fins is one-half of that of the tube having a longitudinal fin.

Heat transfer in the membrane water wall of a CFB boiler can be improved by adding longitudinal fin on the tube surface. For the tubes having the same configuration and dimensions as the test tubes, there is no significant effect from the fin orientation on heat transfer rate. However, the fin orientation has a strong effect on the heat transfer coefficient of the longitudinal fin portion and the combination of tube and membrane fins portion. Heat transfer coefficient of the longitudinal fin at the tube crest is higher than that at 45° from the tube crest. The membrane tube with two longitudinal fins at 45° on both sides of the tube crest has higher heat transfer coefficient of the combination of tube and membrane fins than that of the tube with a longitudinal fin at the tube crest. The membrane tube has highest heat transfer coefficient. The tube with two longitudinal fins tends to have higher heat transfer coefficient than the tube with a longitudinal fin. In addition, the results show that heat is mainly transferred through the combined portion of tube and membrane fins.

As the fin height has an influence on heat transfer from horizontal tubes in a fluidized bed [23], the effect of the longitudinal fin orientation should be investigated for different fin heights in further work.

Acknowledgements

The authors acknowledge the Energy Policy and Planning Office (EPPO): Ministry of Energy, Royal Thai Government for financial support, Postharvest Technology Innovation Center and Instrument Calibration Center (ICC-KKU): Khon Kaen University, Thailand, for their assistance in providing the special tools for fabrication of the experimental rig and performing the instrument calibration, respectively. The authors like to express sincere thanks

to Ian Thomas: Faculty of Science, Khon Kaen University, Thailand for kindly making the manuscript more readable.

References

[1] P. Basu, Combustion and Gasification in Fluidized Beds, CRC Press, FL, 2006.
[2] P. Basu, P.K. Nag, Heat transfer to walls of a circulating fluidized-bed furnace, Chem. Eng. Sci. 51 (1996) 1–26.
[3] L.R. Glicksman, Heat transfer in circulating fluidized beds, in: J.R. Grace, A.A. Avidan, T.M. Knowlton (Eds.), Circulating Fluidized Beds, Chapman & Hall, London, 1997, pp. 261–311.
[4] M.R. Golriz, Influence of wall geometry on local temperature distribution and heat transfer in circulating fluidized bed boilers, in: A. Avidan (Ed.), Circulating Fluidized Bed Technology IV, AIChE, New York, 1994, pp. 693–700.
[5] A. Dutta, P. Basu, An experimental investigation into the heat transfer on wing walls in a circulating fluidized bed boiler, Int. J. Heat Mass Transfer 45 (10) (2002) 4479–4491.
[6] A. Dutta, P. Basu, Overall heat transfer to water walls and wing walls of commercial circulating fluidized bed boilers, J. Inst. Energy 75 (2002) 85–90.
[7] A. Dutta, P. Basu, An investigation on heat transfer to the standpipe of a circulating fluidized bed boiler, Trans IChemE Chem. Eng. Res. Des. 81 (2003) 1003–1014.
[8] A. Dutta, P. Basu, Experimental investigation into cavity type inertial separators – a novel technique fro development of subcompact circulating fluidized bed boilers, Intern. J. Energy Res. 29 (2005) 1279–1300.
[9] R. Zhang, A. Dutta, P. Basu, Heat transfer to the ceiling of the riser of a circulating fluidized bed, Chem. Eng. Sci. 61 (2006) 5907–5911.
[10] P. Basu, L. Cheng, An experimental and theoretical investigation into the heat transfer of a finned water wall tube in a circulating fluidized bed boiler, Int. J. Energy Res. 24 (2000) 291–308.
[11] C. Lockhart, J. Zhu, C.M.H. Brereton, C.J. Lim, J.R. Grace, Local heat transfer, solids concentration and erosion around membrane tubes in a cold model circulating fluidized bed, Int. J. Heat Mass Transfer 38 (13) (1995) 2403–2410.
[12] B.V. Reddy, P.K. Nag, Effect of lateral and extended fins on heat transfer in a circulating fluidized bed, Int. J. Heat Mass Transfer 41 (1) (1998) 139–146.
[13] O. Molerus, Arguments on heat transfer in gas fluidized beds, Chem. Eng. Sci. 48 (1993) 761–770.
[14] R.L. Wu, C.J. Lim, J. Chaouki, J.R. Grace, Heat transfer from a circulating fluidized bed to membrane waterwall surfaces, AIChE J. 33 (1987) 1888–1893.
[15] J.C. Furchi, L. Goldstein Jr., G. Lombardi, M. Mohseni, Experimental local heat transfer in a circulating fluidized bed, in: P. Basu, J.F. Large (Eds.), Circulating Fluidized Bed Technology II, Pergamon Press, Oxford, 1988, pp. 263–270.
[16] P. Basu, T. Ngo, Effect of some operating parameter on heat transfer to vertical fins in a circulating fluidized bed furnace, Powder Technol. 74 (1993) 249–258.
[17] A. Sekthira, Y. Leey, W.E. Genetti, Heat transfer in a circulating fluidized bed, in: 25th International Heat Transfer Conference, Houston, TX, 1988, pp. 24–27.
[18] W. Luan, B.D. Bowen, C.J. Lim, C.M.H. Brereton, J.R. Grace, Suspension-to-membrane-wall heat transfer in a circulating fluidized bed combustor, Int. J. Heat Mass Transfer 43 (2000) 1173–1185.
[19] P.K. Nag, M. Nawsher, P. Basu, A mathematical model for the predicted of heat transfer from finned surfaces in a circulating fluidized bed, Int. J. Heat Mass Transfer 38 (1995) 1675–1681.
[20] M.N. Özişik, Heat Transfer: A Basic Approach, McGraw-Hill, 1985. pp. 73–76.
[21] A.J. Wheeler, A.R. Ganji, Introduction to Engineering Experimentation, second ed., Pearson Prentice Hall, New Jersey, 2004. pp. 180-221.
[22] B.D. Bowen, M. Fournier, J.R. Grace, Heat transfer in membrane waterwalls, Int. J. Heat Mass Transfer 34 (1991) 1043–1057.
[23] W.J. Bartel, W.E. Genetti, Heat transfer from a horizontal bundle of bare and finned tubes in an fluidized bed, AIChE Symp. Ser. (1973) 85–93.